

Retraction

Retracted: Construction of a Multimodal Neuroimaging Data Fusion System and Evaluation of Mental Fatigue Using Nonlinear Analysis

Complexity

Received 23 January 2024; Accepted 23 January 2024; Published 24 January 2024

Copyright © 2024 Complexity. This is an open access article distributed under the Creative Commons Attribution License, which permits unrestricted use, distribution, and reproduction in any medium, provided the original work is properly cited.

This article has been retracted by Hindawi following an investigation undertaken by the publisher [1]. This investigation has uncovered evidence of one or more of the following indicators of systematic manipulation of the publication process:

- (1) Discrepancies in scope
- (2) Discrepancies in the description of the research reported
- (3) Discrepancies between the availability of data and the research described
- (4) Inappropriate citations
- (5) Incoherent, meaningless and/or irrelevant content included in the article
- (6) Manipulated or compromised peer review

The presence of these indicators undermines our confidence in the integrity of the article's content and we cannot, therefore, vouch for its reliability. Please note that this notice is intended solely to alert readers that the content of this article is unreliable. We have not investigated whether authors were aware of or involved in the systematic manipulation of the publication process.

Wiley and Hindawi regrets that the usual quality checks did not identify these issues before publication and have since put additional measures in place to safeguard research integrity.

We wish to credit our own Research Integrity and Research Publishing teams and anonymous and named external researchers and research integrity experts for contributing to this investigation.

The corresponding author, as the representative of all authors, has been given the opportunity to register their agreement or disagreement to this retraction. We have kept a record of any response received.

References

- [1] R. Chen, Z. Li, and Y. Lai, "Construction of a Multimodal Neuroimaging Data Fusion System and Evaluation of Mental Fatigue Using Nonlinear Analysis," *Complexity*, vol. 2021, Article ID 8478868, 13 pages, 2021.

Research Article

Construction of a Multimodal Neuroimaging Data Fusion System and Evaluation of Mental Fatigue Using Nonlinear Analysis

Rui Chen , Zhenzhong Li, and Yi Lai

School of Communications and Information Engineering, Xi'an University of Posts and Telecommunications, Xi'an 710121, China

Correspondence should be addressed to Rui Chen; chenrui@xupt.edu.cn

Received 29 April 2021; Revised 24 May 2021; Accepted 30 May 2021; Published 9 June 2021

Academic Editor: Zhihan Lv

Copyright © 2021 Rui Chen et al. This is an open access article distributed under the Creative Commons Attribution License, which permits unrestricted use, distribution, and reproduction in any medium, provided the original work is properly cited.

The purpose of this research is to explore the optimization and fusion application of multimodal neuroimaging technology and analyze the evaluation method of human brain fatigue based on multimodal neuroimaging technology. Based on electroencephalogram (EEG) and fMRI (functional magnetic resonance imaging), the four-dimensional consistency of local neural activities (FOCA) and local multimodal serial analysis (LMSA) are first introduced to fuse EEG and fMRI organically. Second, the eigenspace maximal information canonical correlation analysis (emiCCA) is introduced to construct the multimodal neuroimaging data fusion system. Finally, how the brain function network is constructed is introduced. Based on the binary and the weighted brain function networks, the relationship between the human brain fatigue and the brain function network is evaluated by calculating the fractal dimension. Results demonstrate that FOCA performs well in temporal and spatial consistency indexes, and the mean level and standard deviation in the case of temporal and spatial consistency are approximately 0.45. The effect of LMSA indexes is significantly better than generalized linear models (GLMs). Under different signal-to-noise ratios (SNRs), the regression coefficient based on LMSA is much larger than the GLM estimate; the corresponding significance level is $p < 0.05$; and the maximum value of the regression coefficient appears near 0.2. In the data fusion system, the time-space matching has good results under the time accuracy based on EEG and the space accuracy based on fMRI, with the time accuracy above 88% and the space accuracy above 89%. The fractal dimension analysis based on the brain function network reveals that the weighted brain function network is more sensitive to mental fatigue. The state of human brain fatigue will make the brain function network more complicated. The fractal dimension with more network edges is around 2.2, while the fractal dimension with fewer network edges is around 1.6. The proposed data analysis and fusion system have great application potential and propose a new idea for analyzing human brain fatigue and brain aging.

1. Introduction

During the developmental process of neuroimaging technology, the single-modality neuroimaging technology was initially the most widely used technology. The fusion of multimodal neuroimaging technology and the integration of data information of different modalities have been initiated as the magnetic resonance imaging (MRI) technology matures [1–3]. As neuroimaging technology develops, researches on functional MRI (fMRI) and electroencephalogram (EEG) occupy the majority [4, 5].

Zhang et al. proposed a time-varying network analysis method based on an adaptive directed transfer function, which was utilized to analyze and discuss the dynamic brain network model during epileptic seizures; the results showed that this time-varying network analysis could better indicate the pathogenesis of epilepsy than EEG and fMRI [6]. Yao et al. proposed that MRI and EEG had low sensitivity and specificity while diagnosing sporadic Creutzfeldt–Jakob disease (sCJD); in contrast, the sensitivity and specificity of real-time quaking-induced conversion (RT-QuIC) were above 95% while diagnosing the same disease [7]. Sharma

et al. applied MRI and EEG technologies to analyze and discuss the symptoms of CJD [8]. Therefore, the single-modality neuroimaging technology, i.e., EEG and fMRI, are no longer applicable in the diagnosis and symptom analysis of many diseases.

To overcome the limitations of single-modality neuroimaging technology, scholars have researched and explored the integration of the two methods. Dhiman found in the discussion of the pathogenesis of hereditary epilepsy patients that the fusion of MRI and EEG technology would be an effective means of implementation [9]. Lu et al. proposed a method that could simultaneously record EEG and fMRI signals and convert the recorded signals into EEG-fMRI music through the Jansen–Rit neural network model, thereby realizing the organic fusion of EEG and fMRI neural imaging technologies [10]. In summary, for the data fusion of multimodal neuroimaging technologies, research results vary. Research on EEG-fMRI data fusion is the most extensive; however, research that simultaneously considers temporal and spatial dimensions is rare.

The problem of mental fatigue becomes increasingly serious as market competition intensifies, and the pace of production and life accelerates. The aggravation of mental fatigue causes a series of problems, such as reduced work efficiency and traffic accidents [11]. Therefore, the analysis of mental fatigue is necessary. The human brain is a complex nonlinear system. Being in a fatigued state for a long time will accelerate brain aging. EEG signal can reflect brain activities, making it widely accepted in mental fatigue evaluation. The evaluation of mental fatigue based on EEG signals includes linear and nonlinear indexes. The former is generated by EEG power ratio, while the latter includes complexity and relevant dimensions. However, traditional mental fatigue evaluation methods based on EEG signals cannot analyze the overall state of the human brain; also, it is difficult for them to reveal the connections between different brain regions. The brain function network uses mutual information to measure the connection of different regions. It can also analyze the weights in different periods, including the resting state and the task state, which overcomes the shortcomings of traditional methods [12]. Many researchers have explored mental fatigue evaluation. Foong et al. analyzed the efficacy of neuromotor therapy in promoting the rehabilitation system. They found that the existence of EEG was correlated with mental fatigue during the use of the brain-computer interface [13]. Under different cognitive loads, Chen et al. adopted fMRI to measure the impact of mental fatigue on brain activation. They evaluated the mental fatigue before and after each behavioral task using the visual simulation fatigue scale. Results suggested a close relationship between the allocation efficiency of neural resources and the aggravation of mental fatigue [14]. In summary, the mechanism of mental fatigue is complicated. Neuroimaging technology can monitor the human brain to some extent. At present, the theory of brain function network is introduced into the evaluation and analysis of mental fatigue; however, the nonlinear analysis of mental fatigue is rarely reported.

In this regard, to explore the data fusion in multimodal neuroimaging technology and seek a feasible method of evaluating human brain fatigue, the four-dimensional consistency of local neural activities (FOCA) and local multimodal serial analysis (LMSA) are first introduced to construct the EEG-fMRI multimodal neuroimaging data fusion system. Then, the brain function network and fractal dimension are introduced based on the evaluation of the human brain fatigue state. The aims are to provide feasible directions for developing and applying neuroimaging technology and explore the relationship between fractal theory and brain function networks.

The main contributions are as follows: (1) creatively, a multimodal neuroimaging data fusion system that integrates EEG, fMRI, and emiCCA is proposed, and its effectiveness in time-space matching is proved and (2) a method that can evaluate the relationship between human brain fatigue and brain function network is introduced based on the fractal dimension; this method can provide good sensitivity, pointing out a possible direction for human brain fatigue evaluation.

2. Methodology

2.1. Temporal and Spatial Data Mining of Human Brain Based on FOCA under EEG-fMRI Fusion. At present, the shared fusion of spatial data information mainly uses MRI data to provide information with higher spatial resolution, which offers very accurate spatial data information for EEG source positioning. Comprehensively, the major problem that still exists in the sharing and fusion of spatial information lies in the difference in spatial position between EEG and fMRI technologies [15]. From the perspective of temporal information sharing and fusion, since the EEG technology shows excellent performance in temporal resolution, the integration of data information in the time dimension should use EEG to provide fMRI with data information at the same time [16]. On the temporal level, the major limitation of the fusion between EEG and fMRI is the difference in their temporal resolutions. From the perspective of temporal-spatial information sharing and fusion, scholars are willing to put more emphasis on the integration of multimodal temporal-spatial information, in which the model-driven and nonmodel-driven are the two most frequently used data fusion methods [17–19]. The data collection of EEG and fMRI neuroimaging technologies is shown in Figure 1.

For fMRI imaging technology, to realize the mining of local temporal-spatial data information of the human brain nerves, the FOCA index is utilized. To obtain the algorithm of the FOCA index, the temporal correlation coefficient is calculated as follows:

$$C_t = \left| \frac{\sum_{i < j}^N r_{ij}^t}{N} \right|; \quad (1)$$

$$N = \frac{k(k-1)}{2},$$

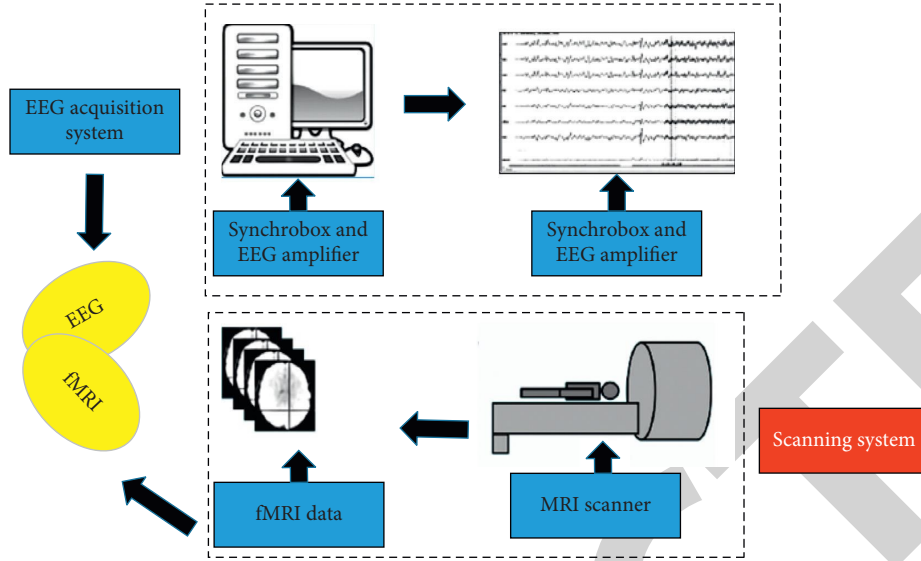


FIGURE 1: Data collection of EEG and fMRI neuroimaging technologies.

where r_{ij}^t corresponds to the Pearson correlation coefficient between the voxel i and time series j , and k corresponds to the corresponding number of voxels locally. For the m -th corresponding time point, the local spatial correlation coefficient of the corresponding adjacent time point is calculated as follows:

$$\bar{r}_m^s = \frac{r_{m,m-1}^s + r_{m,m+1}^s}{2}, \quad (2)$$

where r corresponds to the Pearson correlation coefficient. For all time points, the corresponding average spatial correlation coefficient is calculated as follows:

$$C_s = \frac{\left| \sum_{m=1}^{N_t} \bar{r}_m^s \right|}{N_t}, \quad (3)$$

where N_t characterizes the number of time points. On this basis, the expression and calculation for FOCA values are defined as follows:

$$\text{FOCA} = C_t * C_s. \quad (4)$$

According to the above equation, the FOCA image of the entire human brain nerve is obtained through the numerical calculation of FOCA. Considering the differences between individuals, the FOCA image is defined as follows:

$$\text{FOCA}_{\text{norm}} = \frac{\text{FOCA}}{\text{mean}(\text{FOCA})}. \quad (5)$$

Furthermore, in the simulation analysis of FOCA, the number of voxels is set to 25; the repetition time is set to 2 s; and the number of time points is set to 250. The design and implementation of the simulation experiment are shown in Figure 2.

Figure 2 presents four different time-series characteristics: time consistency, space consistency, time-space consistency, and time-space inconsistency, which can reflect the local spatial activity state under four different

situations. The entire simulation experiment is simulated and generated in a $5 * 5$ grid. Specifically, for these four different situations, time consistency means that changes in activities based on time history are basically the same, while the state of space activities in the near-time state is inconsistent. Space consistency suggests that changes in activities in the time history are basically the same, while the state of space activities at the nearby time point is inconsistent. The other two cases can be deduced by analogy. Furthermore, to organically fuse EEG and fMRI information data and promote the effective acquisition of human brain function data, the index of LMSA is introduced, thus achieving the fusion analysis and characterization of local human brain data information. The fMRI data are expressed as follows:

$$Y \in R^{M \times N}, \quad (6)$$

where M represents the corresponding number of time points, and N represents the corresponding number of voxels. For the activation value corresponding to the i -th voxel, the corresponding calculation is as follows:

$$y_i = [v_i \nu_{\text{cov}}] * [\beta_i \beta_{\text{cov}}] + \varepsilon, \quad (7)$$

where i represents the i -th voxel, β_i represents the regression coefficient of a single element, β_{cov} represents the regression coefficient of the column vector, v_i represents the typical correlation variable of the maximum correlation coefficient corresponding to EEG and fMRI, ν_{cov} represents the covariate matrix including interfering signals such as linear drift, and ε represents the residual value. The calculation of the regression coefficient is as follows:

$$[\hat{\beta}_i \hat{\beta}_{\text{cov}}] = [v_i \nu_{\text{cov}}]^+ * y_i, \quad (8)$$

where $[\cdot]^+$ represents the inverse operation. Finally, by repeating the above calculations for all voxels, a regression

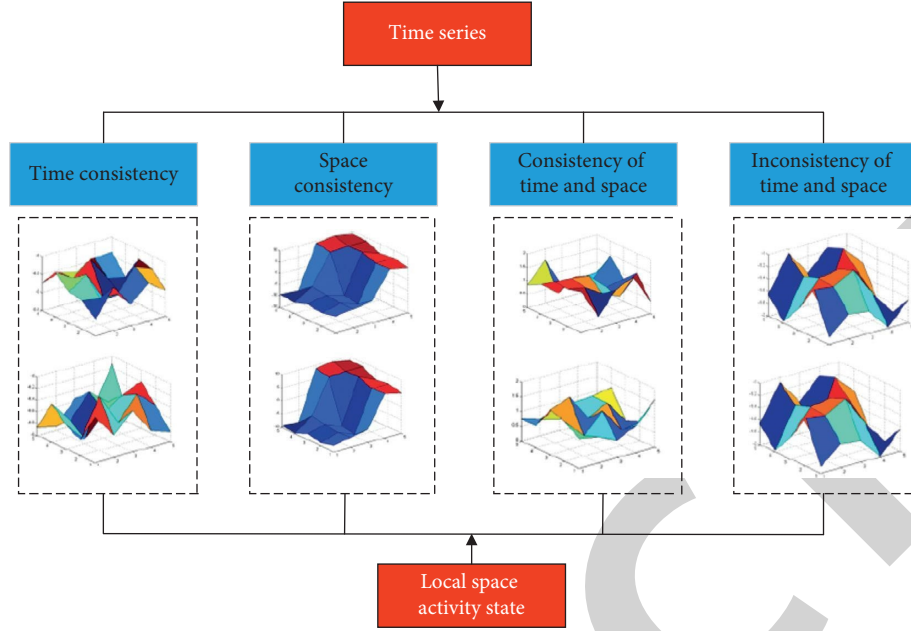


FIGURE 2: Design of fMRI simulation experiment based on FOCA index.

coefficient image of the entire brain is obtained. Correspondingly, the expression and calculation are as follows:

$$t = \frac{\hat{\beta}}{SE(\hat{\beta})}, \quad (9)$$

where $SE(\cdot)$ represents the value of the standard deviation corresponding to $\hat{\beta}$.

Through the above-mentioned calculation and algorithm flow, the information data of EEG and fMRI are organically fused with the LMSA index. To test the LMSA method, the fMRI time series is set to 250; the repetition time is also set to 2 s; and the signal-to-noise ratio is set to 0.1. After 50 repeated calculations, the average result of the simulation analysis is obtained, thereby analyzing the fusion effect of EEG and fMRI information data.

2.2. Construction of the Multimodal Neuroimaging Data Fusion System. For EEG and fMRI neuroimaging technologies, only a single spatial information registration cannot ensure that the components of EEG and fMRI are the same event. In addition to the difference between EEG and fMRI in the time dimension, the registration may fail [20, 21]. Besides, in the process of data information fusion between EEG and fMRI, in addition to paying attention to the shared data information of the two modalities, at the same time, the uncertainty of shared data information should be minimized. From the perspective of data information sharing, the data fusion between EEG and fMRI indicates the same active time course in the same spatial position. Thus, time and space registrations are necessary. On this basis, according to the multimodal data fusion method, a data fusion system that can distinguish the difference between time and space is built. In this system, different time and space data fusion methods are adopted for the registration between modalities.

At the same time, the system also includes multiple layers of credibility from time-space misregistration to time-space registration. The realization of the shared multimodal neuroimaging data fusion system is shown in Figure 3.

To realize the effective analysis of the data fusion system of data EEG and fMRI neuroimaging, the unsupervised learning method is utilized, and the index of eigenspace maximal information canonical correlation analysis (emiCCA) is introduced, which evaluated both the linear and nonlinear correlations among the data. The realization of this analysis index is based on the replacement of correlation coefficient by maximal information coefficient (MIC). First, the corresponding expression and calculation of the MIC coefficient are defined as follows:

$$\phi(X_i; Y_j) = \max_{|X_i||Y_j| < B} \left\{ \frac{I^*(X_i; Y_j)}{\log_2 \left\{ \min \left\{ |X_i|, |Y_j| \right\} \right\}} \right\}, \quad (10)$$

where X_i and Y_j represent the frequency distribution of $X_i - Y_j$ falling in a grid, $I^*(\cdot; \cdot)$ represents the maximum mutual information corresponding to the grid division at a certain resolution, and $|X_i||Y_j| < B$ characterizes that the resolution of the corresponding grid is smaller than the B value. Furthermore, through the above equation, the MIC matrix is obtained, and its corresponding expression and calculation are as follows:

$$\Phi = \begin{pmatrix} \Phi_{X,X} & \Phi_{X,Y} \\ \Phi_{Y,X} & \Phi_{Y,Y} \end{pmatrix}. \quad (11)$$

If the weight vectors α and β meet the following conditions

$$\text{maximize}_{\alpha, \beta} \alpha^T \Phi_{X,Y} \beta, \quad (12)$$

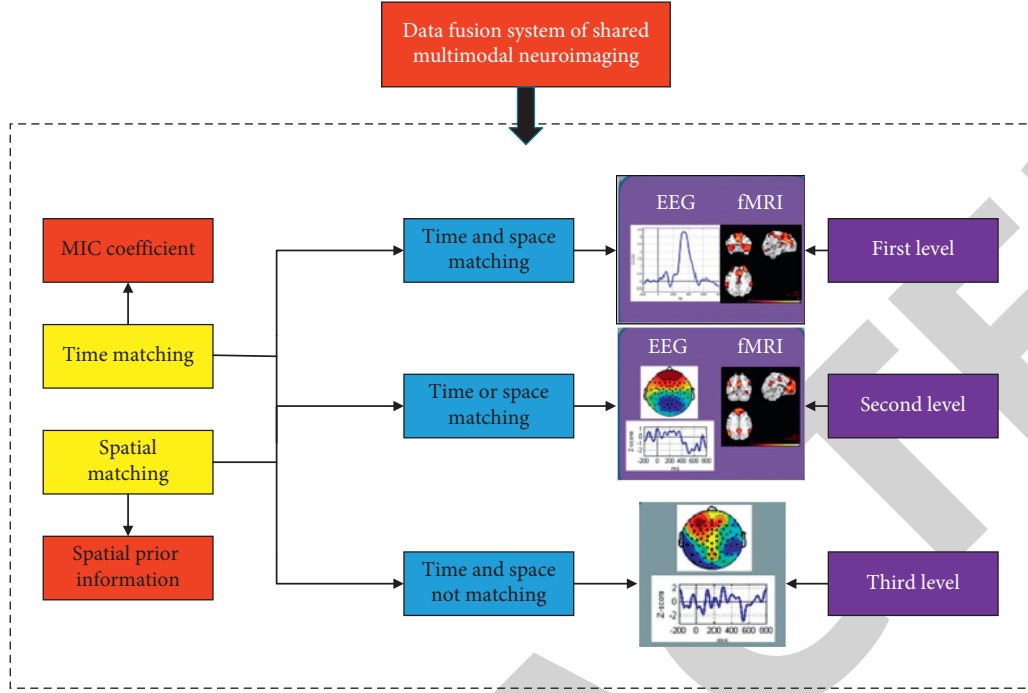


FIGURE 3: Realization of neuroimaging data fusion system based on shared multimodal.

where α and β correspond to the weight vectors of feature spaces X and Y . With the help of α and β , each variable in the corresponding data set is quantified to show the correlations among the data sets. The square root of the positive number corresponding to the eigenvalue in Equation (12) above is actually emiCCA. While emiCCA is tested, the number of data points is set to 1600 and the data dimensions are set to (3, 2), (6, 4), (12, 8), (18, 12), (24, 16), and (30, 20). To explore the impact of the number of data points and noise, the corresponding functional correlations among variables are, respectively, linear function (F1), quadratic function (F2), absolute value function (F3), cosine function (F4), exponential function (F5), circular equation (F6), inseparable function (F7), equation (F8), and independent random variable (F9). Besides, in the case of noise, the emiCCA method under different function variables as well as the linear CCA (ICCA) method and the kernel CCA (kCCA) method are compared and investigated.

The implementation of this system has gone through four stages, i.e., weight extraction, time registration, space registration, and time-space registration. First, in the weight extraction stage, the independent component analysis (ICA) method is used [22, 23]. Besides, the temporal and spatial ICA is used to decompose the EEG and fMRI information data. The corresponding expressions and calculations are as follows:

$$\begin{aligned} Y_e &= B_e^{n_1 * p} T_e^{p * m_1} + \varepsilon_e, \\ Y_f &= B_f^{n_2 * q} T_f^{q * m_2} + \varepsilon_f, \end{aligned} \quad (13)$$

where Y_e represents the EEG-related data at the trial level, n_1 represents the conductive electrode, m_1 represents the corresponding time point, Y_f represents the relevant data

after fMRI preprocessing, B_e represents the EEG space map after decomposition, B_f represents the spatially independent components, and ε corresponds to the residual. Furthermore, the amplitude of EEG-related events is expressed and calculated by the following equation:

$$Z_e = (T_e \{t'\}), \quad (14)$$

where t' represents the time point corresponding to the maximum amplitude.

The single amplitude calculation of fMRI is achieved in two steps. One is the calculation of the hemodynamic response function (HRF) of the fMRI time series, which is defined as follows:

$$\text{HRF} = M^+(T_f)^T, \quad (15)$$

where M^+ represents the generalized inverse corresponding to the convolution matrix, and T_f represents the time series. The second is the calculation of the horizontal amplitude of a single trial of the corresponding time series of fMRI, which is defined as follows:

$$\begin{aligned} (T_f)^T &= (D \otimes \text{HRF})Z_f + \varepsilon, \\ Z_f &= (D \otimes \text{HRF})^+(T_f)^T, \end{aligned} \quad (16)$$

where D represents the design matrix corresponding to the start time of a single trial, \otimes represents the convolution operation, Z_f represents the amplitude of time-series-related events, and ε corresponds to residuals.

Through the above calculations and corresponding definitions, the amplitude sequence corresponding to EEG and fMRI is finally obtained, which indicates the related dynamic changes of EEG and fMRI. According to different

repetition times, the hemodynamic response functions (HRFs) are divided and compared with HRF-1, HRF-2, HRF-3, and HRF-4, and their corresponding repetition times are 0, 1.5, 3, and 4, respectively.

In the temporal registration stage, the MIC is used to complete the time registration between EEG and fMRI. The corresponding calculation is as follows:

$$\text{MIC}(z_1; z_2) = \max_{|z_1||z_2| < G} \left\{ \frac{I^*(Z_1; Z_2)}{\log_2 \{ \min\{|Z_1|, |Z_2|\} \}} \right\}, \quad (17)$$

where Z_1 and Z_2 correspond to the frequency distribution that falls in a grid, $I^*(\cdot; \cdot)$ represents the maximum mutual information under a certain grid, and $|z_1||z_2| < G$ represents that the resolution ratio of the grid is smaller than G .

In the spatial registration stage, for the location analysis of the EEG source, the parameter empirical Bayes model is used, and the corresponding expression and calculation are as follows:

$$\begin{aligned} B_e^{(i)} &= L_e \Phi_e + E_{1e}, \\ \Phi_e^{(i)} &= 0 + E_{2e}, \end{aligned} \quad (18)$$

where $B_e^{(i)}$ represents the i -th EEG topographic map, L_e represents the transfer matrix of the known head model, $\Phi_e^{(i)}$ represents the source distribution corresponding to the unknown dipole, and E_{1e} and E_{2e} correspond to the random terms between the electrode and the source spatial level. Furthermore, the expression and calculation of the prior information of covariance are as follows:

$$C_{2e} = \sum_{i=1}^q \gamma_i V \{ B_f^{(i)} \} + \sum_{j=1}^l \gamma_j V \{ \text{MSP}^{(j)} \}, \quad (19)$$

where γ represents a hyperparameter and has a nonnegative value, V represents a covariance basis matrix, B_f represents a spatially independent component corresponding to fMRI, and MSP represents a sparse source.

In summary, in the constructed multimodal neuroimaging data fusion system, temporal registration is achieved through MIC coefficients, and spatial registration is achieved through spatial prior information. Each area in the system is divided into five component sources, which are recorded as visual area (S1), default network (S2), auditory cortex (S3), left-hand cognition (S4), and right-hand cognition (S5). The simulation data set used is randomly generated through standard uniform distribution to analyze the performance of emiCCA, ICCA, and kCCA. The number of data points used for analysis is set to 1200; the dimension of data set X is set to 6, and the dimension of data set Y is set to 4. On this basis, different data dimensions are set to test the influence of data dimensions on emiCCA, ICCA, and kCCA.

2.3. Fractal Dimension and Calculation Improvement of Complex Networks. Fractals originally represented phenomena or processes with self-similar characteristics, whose original indications were irregularities and fractions. There

is no definite meaning for fractal at present. However, despite the definitions, self-similarity, scale-freeness, and self-affinity are the foremost characteristics of a fractal. Fractals exist extensively in nature and society; thus, they can be divided into four types: natural fractal, time fractal, social fractal, and thinking fractal.

Dimension is a fundamental concept in geometry. However, it is difficult to describe natural objects such as mountains using conventional geometric features. The fractal dimension can quantitatively describe the basic composition parameters, which analyzes the irregularity and complexity of the object. There is a positive correlation between the size of the fractal dimension and the complexity of the described object. The fractal features of a complex network represent the self-similarity of the network structure, which can measure the degrees of irregularity and complexity of the network. Complex networks include social relationship networks and cellular networks. Research on the fractal features of complex networks mainly adopts the geometric method based on the box covering and the algebraic method based on spectral analysis, in which the box covering method can be described as follows:

$$n_b \approx l_b^{-d_b}, \quad (20)$$

where n_b represents the number of boxes that can cover the entire network, l_b represents the size of the box, and d_b represents the dimension of the box in the complex network.

However, when calculating the fractal dimension d_b using the above equation, finding the smallest number of boxes is one of the difficulties. In this regard, a greedy coloring algorithm is proposed by improving the box covering method. The difference is that each box in the greedy coloring algorithm does not need a central node, and all the nodes in a box present a random arrangement. According to the box covering method, if the size of the box given for a network N is $l_b = 3$, the shortest path in the network will be connected, that is, nodes with a distance of three are connected to obtain network N_1 . Then the newly obtained network is colored to make the nodes that are connected to each other have different colors, and a new network N_2 can also be obtained from this. After the coloring operation is completed, the new network N_3 can be obtained once the initial connection is restored. The number of color types corresponding to the new network is the number of boxes n_b required to determine the box size in the overall network. To calculate the fractal dimension in the complex network, first, all the nodes are randomly numbered. For the determined box size l_b , the color corresponding to the first node is assigned a value of 0, and the box size is set to $l_b = 1$. Then the distance between the current node i and the remaining node j is calculated. If all nodes satisfy $l_{ij} \geq l_b$, one of the nodes is selected as the unused color under the current box size l_b , which is regarded as the color value c_{ill} corresponding to the node i . The above steps are repeated until $l_b = l_b^{\max}$ is satisfied. The number of color values used in each column is calculated, and the value obtained is the number of boxes n_b needed to cover the overall network under different box sizes. Finally, $\log(l_b)$ and $\log(n_b)$ are fitted, and the obtained

absolute value of the slope is the fractal dimension d_b corresponding to the complex network.

2.4. Mental Fatigue Detection and Evaluation Based on emiCCA Nonlinear Index. When constructing the above multimodal neuroimaging data fusion system, nonlinear correlations are considered for the first time based on the index of emiCCA. The human brain is actually a complex nonlinear system; thus, the nonlinear analysis method is accurate in analyzing human brain activities, which is also effective for investigating the characteristics of the human brain. Mental fatigue caused by work performance decline and impaired cognitive level is seriously affecting people's living conditions. Therefore, it is necessary to monitor mental fatigue effectively. In response to this problem, the formation of mental fatigue is analyzed based on the fractal features of the complex network by constructing a brain function network.

Complex networks can be divided into directed and undirected networks or binary and weighted networks where the latter characterizes the network with a weight of 1. Methods to construct the brain function network include valuing a weight and valuing a fixed network's edge number, written as $M1$ and $M2$, respectively. $M1$ can reveal the effect of weight on the network structure. For an adjacency matrix, when the weight as a whole is at a high level, the number of edges corresponding to the brain function network is also large, which can distinguish the network features such as clustering coefficient and global efficiency. $M2$ emphasizes the influence of the network edges' spatial distribution on the network features, which can effectively distinguish the differences in the features of the brain function network. Here, a series of thresholds are taken from $M1$ and $M2$ to analyze the effect of network feature composition on mental fatigue more precisely. The determination of the threshold aims to ensure that no isolated nodes are in the constructed brain function network so that the difference in the network feature composition can be expanded at different time stages.

The greedy coloring algorithm optimized above is used to analyze the fractal characteristics of the brain function network in the process of mental fatigue, and the calculation threshold is set to 0.36. The fractal dimensions of the binary brain function network and the weighted brain function network are analyzed at six different time nodes ($t_0, t_1, t_2, t_3, t_4,$ and t_5), where t_0 represents the initial stage, t_1 to t_5 mean that the human brain is in a state of fatigue, and the degree gradually deepens.

3. Results and Discussion

3.1. Results of FOCA Simulation Analysis. Through the calculation of the temporal correlation coefficient, spatial correlation coefficient, and FOCA value, the simulation analysis results of the FOCA index are shown in Figure 4.

In Figure 4, A to D and A' to D' represent the mean value and the standard deviation, respectively, corresponding to the FOCA index when the time is consistent, the space is

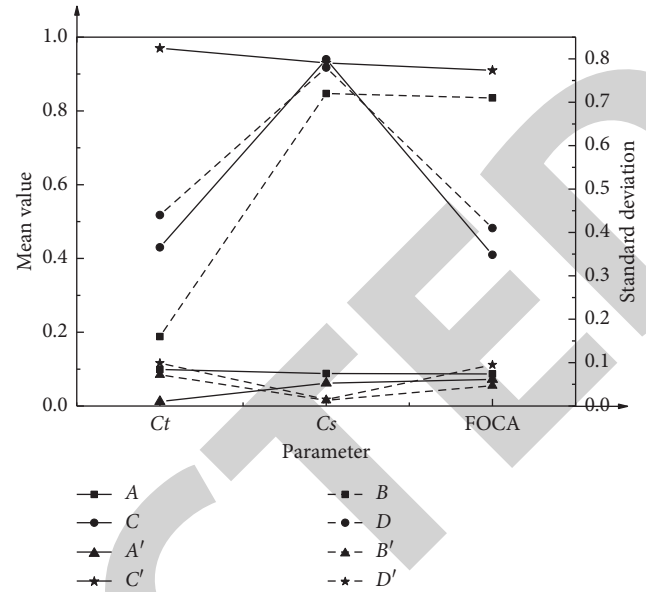


FIGURE 4: Mean and standard deviation simulation analysis results of FOCA index.

consistent, the time space is inconsistent, and the time space is consistent.

As shown in Figure 4, the statistical value corresponding to the FOCA index ranges between the values of the time correlation coefficient (Ct) and the space correlation coefficient (Cs) despite time consistency, space consistency, time-space consistency, or time-space inconsistency. Therefore, under the premise of time-space consistency, Ct , Cs , and FOCA values are the closest. The simulation results in the case of time-space consistency are very stable. Through data analysis, it is found that the FOCA index is well-performed on the temporal and spatial consistencies during the process of local voxel activities. Thus, it is speculated that if this index is used in fMRI neuroimaging technology, it will show and characterize the temporal-spatial consistency characteristics of local regions.

In the indication and representation of the consistency of the characteristics of spontaneous activity related to the local region of the human brain nerve, methods and indexes including local consistency, integrated local correlation, and local functional connection density have been used. However, these traditional indexes still have limitations, such as that the local consistency index method is dependent on voxel size [24]. Pu et al. analyzed the abnormal synchronization of fMRI signals in patients based on FOCA indexes. They found that the overall functional connectivity strength and density of the areas with significant differences in FOCA were different, pointing out directions for the pathophysiological mechanism of patients with abnormal brain function [25]. These findings can support the present work. The FOCA index used fully considers the temporal correlation between voxels in local regions and the spatial correlation between voxels in local regions at adjacent time points. The above analysis results show that if this index method is applied to fMRI neuroimaging technology, it will play an important role in the mining of time-space information of

the spontaneous activity process in the local region of the human brain nerves.

3.2. EEG-fMRI Shared Multimodal Simulation Analysis. Through consideration of different HRF functions, the simulation analysis results for the LMSA method and GLM method under different signal-to-noise ratios are shown in Figure 5.

As shown in Figure 5, the regression coefficients of the both LMSA method and GLM method are positively related to the changes in the signal-to-noise ratios. However, in general, the effect of LMSA is better than that of GLM, and the significance level p is <0.05 . From the perspective of the HRF function, given the differences in signal-to-noise ratio, the regression coefficient obtained by the LMSA method is much larger than the regression coefficient obtained by GLM method. When the HRF function corresponds to HRF-3, the corresponding activation is detected under the different signal-to-noise ratios by the LMSA method; in contrast, it cannot be detected by the GLM method.

Based on the data fusion analysis of EEG and fMRI, the proposed LMSA method fully considers the shared time-related data information between multimodalities and also takes into account the uncertainties in multimodal neuroimaging data fusion. The above simulation analysis results show that the introduction of this method has an important role in solving the problem of low signal-to-noise ratio in the HRF. Therefore, it is expected to solve problems such as human brain nerve function disorders. To promote the maintenance of the healthy state of the human brain nervous system, the proposed method also laid a foundation for the fusion of multimodal data of neuroimaging technologies such as EEG and fMRI. Wu et al. analyzed the relationship between fMRI neuroimaging technology and HRF indicators regarding brain activity in the resting state. They found that combining fMRI and HRF could effectively track the neurovascular coupling [26]. Obviously, this effect becomes more significant under EEG-fMRI fusion.

3.3. Implementation of Multimodal Neuroimaging Data Fusion System. Given different function variables, the changes in corresponding coefficients of the three methods, such as emiCCA, ICCA, and kCCA, are shown in Figure 6. Given different data dimensions and different data points, the time-consuming changes produced by these three methods are shown in Figures 7(a) and 7(b).

According to Figures 6 and 7, despite the linear or nonlinear relationships, the coefficient corresponding to emiCCA is the most significant; however, that corresponding to the independent random variable is not significant. In contrast, ICCA can obtain significant correlation coefficients for quadratic functions and exponential functions, while kCCA provides a corresponding word number of 1 basically for any function. According to the time consumption changes in these three methods, in different data dimensions, the average time consumption corresponding to emiCCA is distributed between those of ICCA and kCCA, showing the same trend under different data

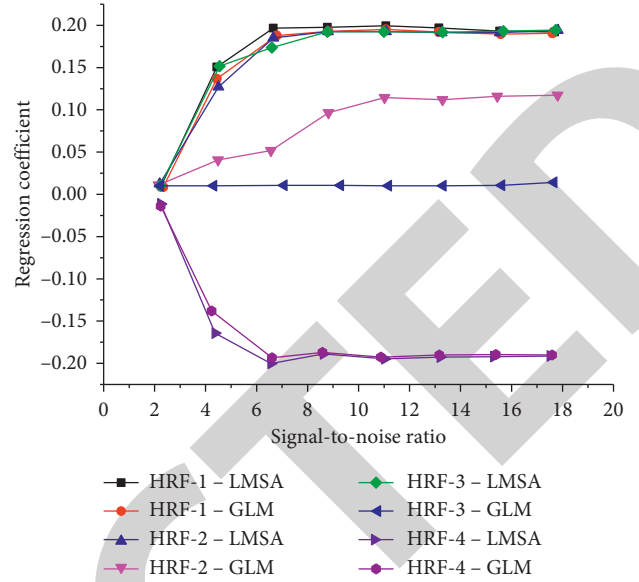


FIGURE 5: Simulation analysis results of LMSA and GLM under different signal-to-noise ratios.

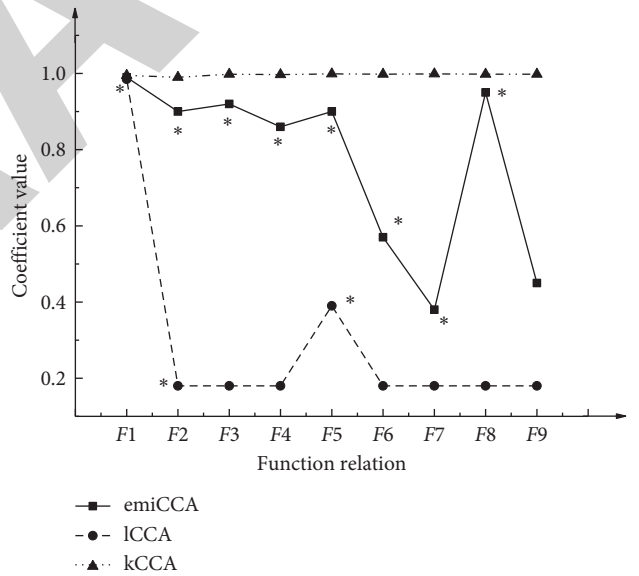


FIGURE 6: Coefficient changes of emiCCA, ICCA, and kCCA corresponding to different function variables.

points. The correlation coefficient and average time consumption results reveal that the emiCCA method has obvious advantages.

Through the temporal registration based on MIC coefficient and the spatial registration based on spatial prior information, the simulation analysis results of EEG temporal registration accuracy and fMRI spatial registration accuracy are obtained, as shown in Figure 8.

Through data analysis, it is found that the components of the temporal-spatial registration show better results in terms of time accuracy based on EEG and spatial accuracy based on fMRI. In contrast, the components in the second level of the

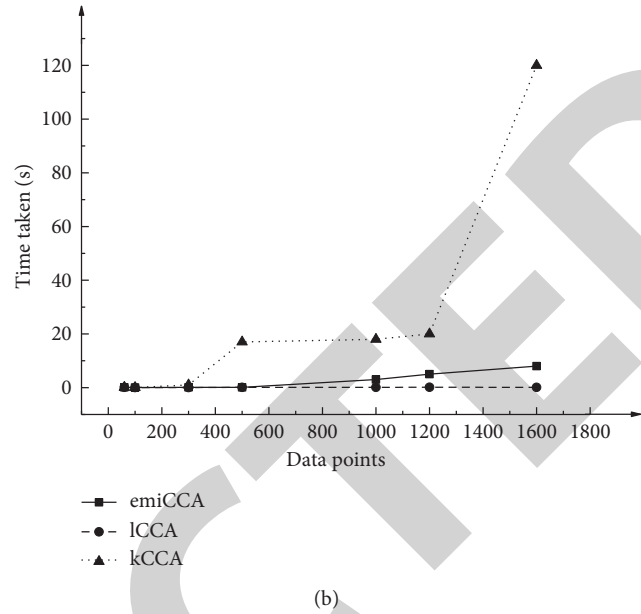
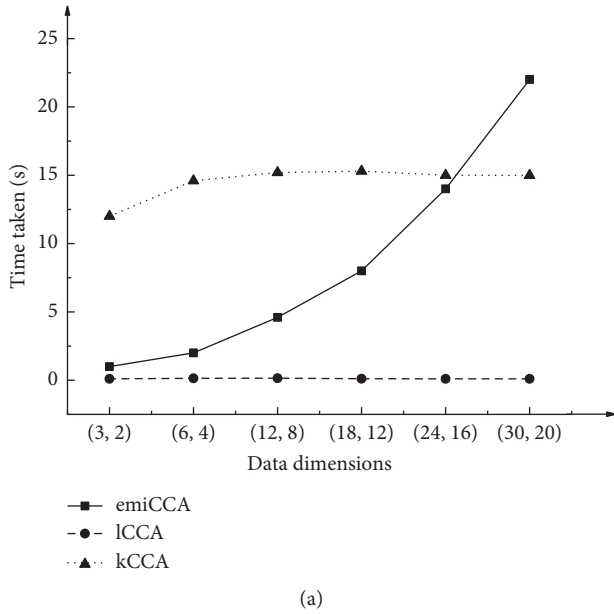


FIGURE 7: Time-consuming changes produced by the emiCCA, ICCA, and kCCA methods: (a) different data dimensions and (b) different data points.

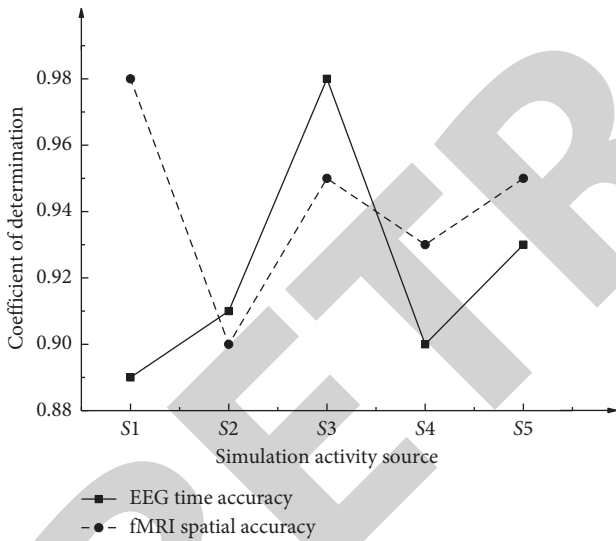


FIGURE 8: Simulation analysis results of EEG temporal registration accuracy and fMRI spatial registration accuracy.

data fusion system only show the advantages of time and space dimensions under single modality.

Based on the problem of registration failures in EEG and fMRI, a multimodal neuroimaging data fusion system is constructed, and a hierarchical data information structure for temporal-spatial registration is proposed. As shown in the simulation analysis results, the construction of the data fusion system makes the data information shared by EEG and fMRI more prominent; at the same time, this system significantly reduces the uncertainty between the corresponding modalities. Jonmohamadi et al. introduced the source space into the fusion of EEG and fMRI neuroimaging technology, revealing its effectiveness in temporal and

spatial data matching [27]. A credible result of level matching can be obtained in the present work based on the fusion method in the first level. Specifically, it can be explained as that the first level of temporal and spatial matching corresponding to EEG and fMRI aims to reveal the most credible component of brain behavior. Unlike the first level, the main function of the second level is to provide supplementary explanatory information.

3.4. Mental Fatigue Evaluation Based on Binary Network Fractal Dimension Analysis. When the calculated threshold is 0.36, the fractal dimension analysis results of the binary brain function network corresponding to different time stages are presented in Figure 9.

In the six different time stages, $\log(l_b)$ and $\log(n_b)$ show better fitting results; moreover, when the degree of mental fatigue increases, the fractal dimension corresponding to the brain function network increases. According to Equation (20), thresholds selected for $M1$ are 0.15, 0.2, and 0.3, and those for $M2$ are 40, 65, and 90, respectively. The corresponding results are the average values obtained after 100 calculations. The calculation results of the fractal dimension in the binary network obtained corresponding to $M1$ and $M2$ are displayed in Figures 10(a) and 10(b).

When the threshold value is 0.32, the fractal dimension corresponding to $M1$ shows a significant change, presenting a correspondence relationship with the results in Figure 9. The fractal dimension of all selection thresholds corresponding to $M2$ has no significant changes in different time stages. Specifically, when the number of network edges is large, the fractal dimension of the corresponding brain function network is about 2.2; when the number of network edges is small, the fractal dimension of the corresponding brain function network is about 1.6. By aiming to evaluate

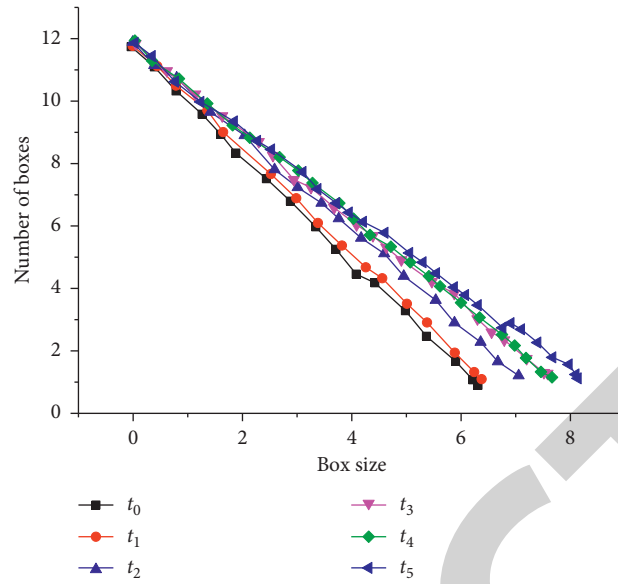


FIGURE 9: The fractal dimension analysis results of the binary brain function network corresponding to different time stages.

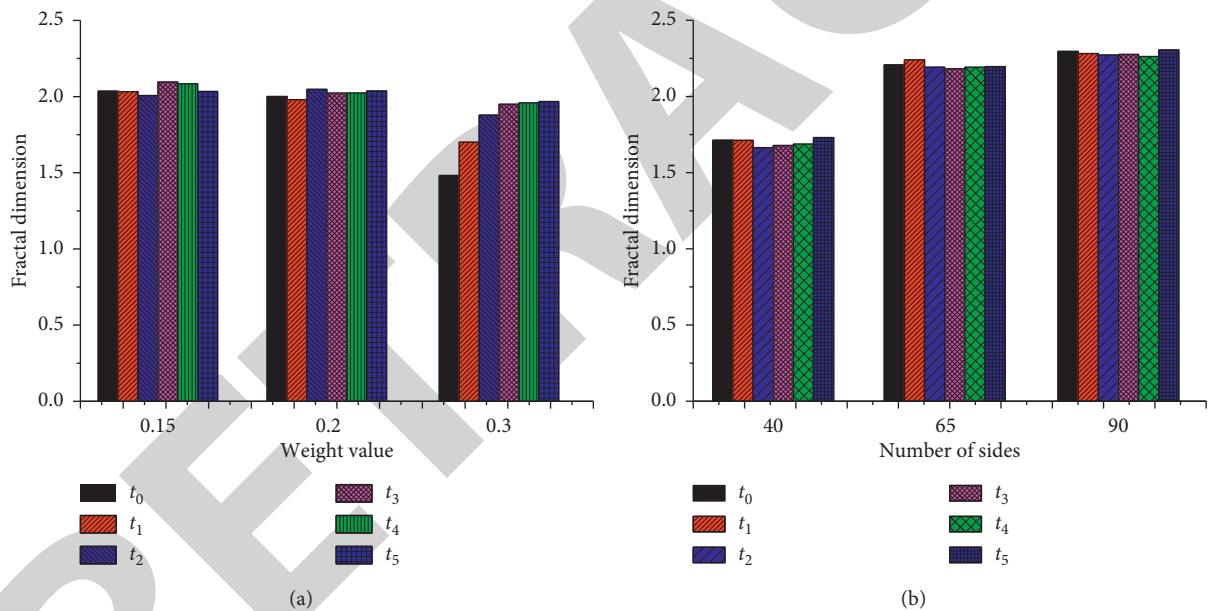


FIGURE 10: The calculation results of the fractal dimension in the binary network based on (a) $M1$ and (b) $M2$.

the brain fatigue state, Li et al. analyzed the influence of mental fatigue on the fractal dimension of the brain function network. They found that the increase in mental fatigue was positively correlated with the fractal dimension, while the fractal dimension of the weighted network was more sensitive to mental fatigue [28]. These results can support the research results in the present work. The difference is that the emiCCA index is introduced in the present work.

3.5. Mental Fatigue Evaluation Based on Weighted Network Fractal Dimension Analysis. When the calculated threshold is 0.36, the fractal dimension analysis results of the weighted

brain function network corresponding to different time stages are presented in Figure 11.

As shown in Figure 11, $\log(l_b)$ and $\log(n_b)$ corresponding to different time stages provide good fitting results. Even if the brain is in a fatigued state, the weighted brain function network can maintain the fractal structure, and the increase in the degree of mental fatigue also shows a positive correlation with the fractal dimension, which is similar to the binary brain function network. In contrast, in the time stages t_3 and t_4 , the fractal dimension in the binary brain function network cannot be distinguished, while in the weighted brain function network, the distinction is noticeable. Thus, the latter can provide better performance in

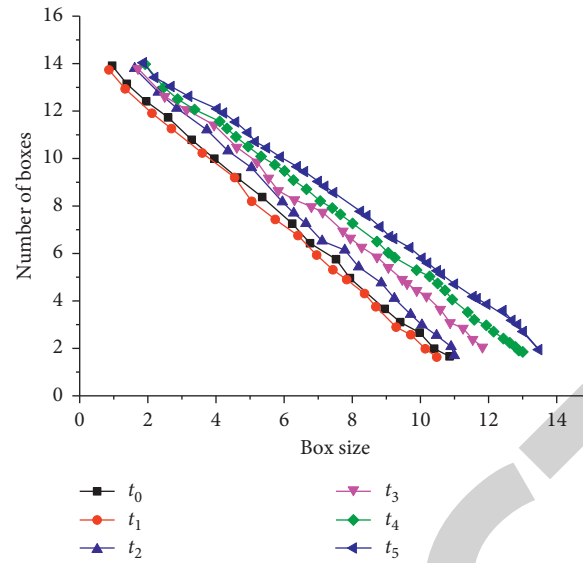


FIGURE 11: The fractal dimension analysis results of the weighted brain function network corresponding to different time stages.

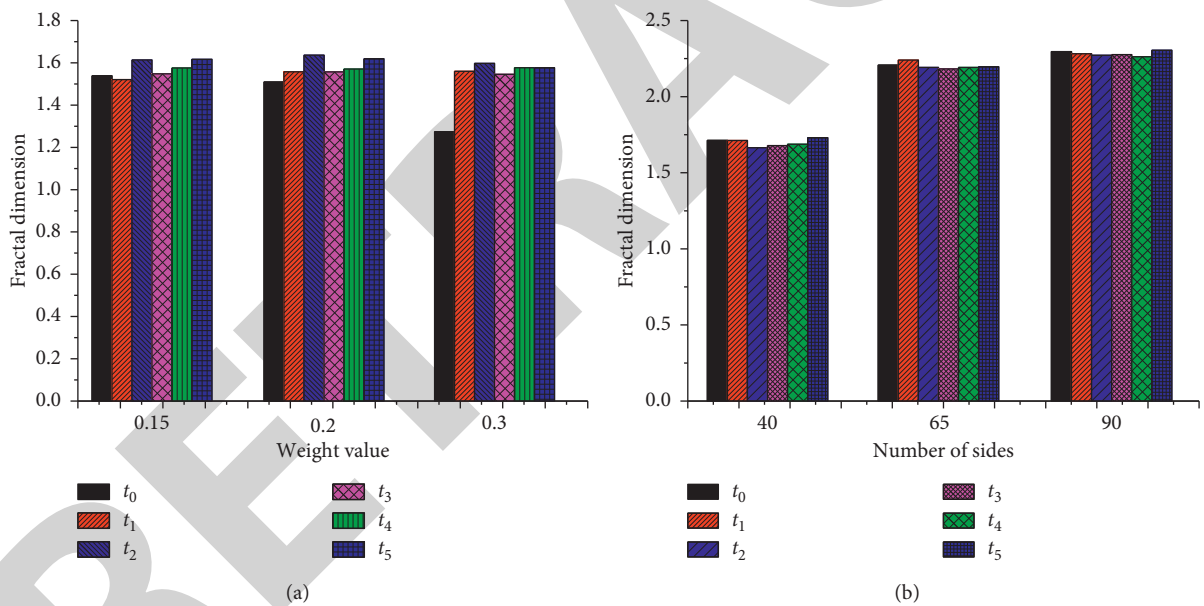


FIGURE 12: The calculation results of the fractal dimension in the weighted network based on (a) $M1$ and (b) $M2$.

this regard. Under the same threshold setting, the calculation results of the fractal dimension corresponding to $M1$ and $M2$ are shown in Figures 12(a) and 12(b).

The increase in mental fatigue degree is positively correlated to the fractal dimension under both $M1$ and $M2$. With the further deterioration of fatigue degree, the fractal dimension corresponding to the weighted brain function network increases. In contrast, $M2$'s description of fractal dimension is better than $M1$, and the changing trend under different time stages also shows good consistency.

The above fractal dimension analysis results based on the binary brain function network and the weighted brain

function network are summarized. $M1$ has a better response to mental fatigue in the binary brain function network because of the number of edges in the network. In the weighted brain function network, $M2$ shows better consistency for mental fatigue because the network weight has a greater effect on the fractal dimension at this time. Briefly, the weighted brain function network is more sensitive to the degree of mental fatigue. This result can also be caused by the more comprehensive coverage of the box size by the weighted brain function network. The fractal dimension can also measure the degree of complexity for self-similar structures. The above analysis suggests that the mental

fatigue state will make the brain function network more complicated, and the increase in this complexity can aggravate the degree of mental fatigue.

4. Conclusion

The research objects are EEG and fMRI neuroimaging technologies. Two dimensions of space and time are introduced. The FOCA based on fMRI optimizes the algorithm indexes. Based on the LMSA index under data fusion, a multilayer and multimodal neuroimaging data fusion system is constructed innovatively. Furthermore, by introducing the idea of fractal dimension, a novel method that can evaluate brain function network is proposed. Through simulation, the introduction of FOCA and LMSA indexes shows a good effect in temporal and spatial voxel activities under the EEG-fMRI fusion, which can well reflect the characteristics of time-space consistency in local areas. The LMSA index comprehensively considers multimodal shared time data and neuroimaging data fusion, making it possible to deal with human brain neurological disorders. The organic fusion of time accuracy based on EEG and spatial accuracy based on fMRI provides effective ideas for dealing with brain function problems. Regarding the responses to human brain fatigue, the weighted brain function network provides excellent performance, and the increase in fractal dimension also reflects the complexity of the brain function network. The research results can provide a direction for developing shared multimodal neuroimaging technology. However, the internal mechanism of FOCA has not yet been involved in the present work; the focus is on the construction of the data fusion system and the combination with the classification theory; nevertheless, the specific practical application has not yet been involved. A more in-depth analysis will be provided for each index, and a more detailed analysis will be performed to evaluate human brain fatigue in future works.

Data Availability

All data are fully available without restriction.

Conflicts of Interest

The authors declare that they have no conflicts of interest.

Acknowledgments

This work was supported in part by the Shaanxi Provincial Natural Science Basic Research Project under grant no. 2019JM-605.

References

- [1] Q. Gong, M. Janowski, H. Tang et al., "Magnetic resonance imaging of the functional anatomy of the superior oblique muscle in patients with primary superior oblique overaction," *Eye*, vol. 31, no. 4, pp. 588–592, 2017.
- [2] H.-f. Tong, H.-b. Liang, Z.-k. Mo et al., "Quantitative analysis of gadoteric acid-enhanced magnetic resonance imaging predicts histological grade of hepatocellular carcinoma," *Clinical Imaging*, vol. 43, pp. 9–14, 2017.
- [3] R. Schmidt, A. Slobozhanyuk, P. Belov, and A. Webb, "Flexible and compact hybrid metasurfaces for enhanced ultra high field in vivo magnetic resonance imaging," *Scientific Reports*, vol. 7, no. 1, p. 1678, 2017.
- [4] S. Kemp, G. Prendergast, T. Karapanagiotidis et al., "Concordance between the wada test and neuroimaging lateralization: influence of imaging modality (fMRI and MEG) and patient experience," *Epilepsy & Behavior*, vol. 78, pp. 155–160, 2018.
- [5] J. Kang, B. J. Reich, and A.-M. Staicu, "Scalar-on-image regression via the soft-thresholded Gaussian process," *Biometrika*, vol. 105, no. 1, pp. 165–184, 2018.
- [6] L. Zhang, Y. Liang, F. Li et al., "Time-varying networks of inter-ictal discharging reveal epileptogenic zone," *Frontiers in Computational Neuroscience*, vol. 11, p. 77, 2017.
- [7] Y. Yao, X. Dong, H. Guan et al., "Cerebrospinal fluid real-time quaking-induced conversion test for sporadic creutzfeldt-jakob disease in an 18-year-old woman: a case report," *Medicine*, vol. 96, no. 48, Article ID e8699, 2017.
- [8] D. K. Sharma, M. Boggild, A. W. van Heuven, and R. P. White, "Creutzfeldt-Jakob disease presenting as stroke: a case report and systematic literature review," *The Neurologist*, vol. 22, no. 2, pp. 48–53, 2017.
- [9] V. Dhiman, "Molecular genetics of epilepsy: a clinician's perspective," *Annals of Indian Academy of Neurology*, vol. 20, no. 2, pp. 96–102, 2017.
- [10] J. Lu, S. Guo, M. Chen et al., "Generate the scale-free brain music from BOLD signals," *Medicine*, vol. 97, no. 2, Article ID e9628, 2018.
- [11] V. Villani, B. Capelli, C. Secchi et al., "Humans interacting with multi-robot systems: a natural affect-based approach," *Autonomous Robots*, vol. 44, no. 12, pp. 1–16, 2020.
- [12] U. Lee, M. Kim, K. Lee et al., "Functional brain network mechanism of hypersensitivity in chronic pain," *Scientific Reports*, vol. 8, no. 1, p. 243, 2018.
- [13] R. Foong, K. K. Ang, C. Quek et al., "Assessment of the efficacy of EEG-based MI-BCI with visual feedback and EEG correlates of mental fatigue for upper-limb stroke rehabilitation," *IEEE Transactions on Biomedical Engineering*, vol. 67, no. 3, pp. 786–795, 2020.
- [14] M. H. Chen, G. R. Wylie, B. M. Sandroff et al., "Neural mechanisms underlying state mental fatigue in multiple sclerosis: a pilot study," *Journal of Neurology*, vol. 267, no. 8, pp. 2372–2382, 2020.
- [15] D. T. Puterbaugh, "What's your excuse?" *USA Today*, vol. 146, no. 2876, p. 82, 2018.
- [16] M. Rashdan, "Dual-time resolution time-based transceiver for low-power serial interfaces," *Analog Integrated Circuits and Signal Processing*, vol. 92, no. 1, pp. 81–89, 2017.
- [17] M. Sargolzaei Javan and M. K. Akbari, "Smartdata 4.0: a formal description framework for big data," *The Journal of Supercomputing*, vol. 75, no. 7, pp. 3585–3620, 2019.
- [18] J. S. Kinnebrew, J. R. Segedy, and G. Biswas, "Integrating model-driven and data-driven techniques for analyzing learning behaviors in open-ended learning environments," *IEEE Transactions on Learning Technologies*, vol. 10, no. 2, p. 1, 2015.
- [19] S. Bernardi, S. Marrone, J. Merseguer et al., "Towards a model-driven engineering approach for the assessment of non-functional properties using multi-formalism," *Software & Systems Modeling*, vol. 18, no. 3, pp. 2241–2264, 2019.
- [20] M. Zieleniewska, A. Duszyk, R. Piotr et al., "Parametric description of EEG profiles for assessment of sleep architecture

- in disorders of consciousness,” *International Journal of Neural Systems*, vol. 29, no. 3, Article ID 1850049, 2019.
- [21] P. Fitzgerald, “EEG and fMRI network-based predictors of response to rTMS in depression,” *Brain Stimulation*, vol. 12, no. 2, pp. 395-396, 2019.
- [22] A. Al-Saegh, “Comparison of complex-valued independent component analysis algorithms for EEG data,” *Iraqi Journal for Electrical and Electronic Engineering*, vol. 15, no. 1, pp. 1-12, 2019.
- [23] E. Damaraju, E. Tagliazucchi, H. Laufs, and V. D Calhoun, “Connectivity dynamics from wakefulness to sleep,” *NeuroImage*, vol. 220, Article ID 117047, 2020.
- [24] D. Leeds, D. Shutov, and J. Pyles, *Local Multi-Voxel Cortical Representations of Object Semantics fMRI and Mechanical Turk Data*, Carnegie Mellon University, Pittsburgh, PA, USA, 2018.
- [25] P. Wang, X. Luo, C. Zhong et al., “Resting state fMRI reveals the altered synchronization of BOLD signals in essential tremor,” *Journal of the Neurological Sciences*, vol. 392, pp. 69-76, 2018.
- [26] G.-R. Wu, C. Di Perri, V. Charland-Verville et al., “Modulation of the spontaneous hemodynamic response function across levels of consciousness,” *NeuroImage*, vol. 200, pp. 450-459, 2019.
- [27] Y. Jonmohamadi, A. Forsyth, R. Mcmillan, and S. D. Muthukumaraswamy, “Constrained temporal parallel decomposition for EEG-fMRI fusion,” *Journal of Neural Engineering*, vol. 16, no. 1, Article ID 016017, 2018.
- [28] G. Li, Y. Xu, Y. Jiang et al., “Mental fatigue has great impact on the fractal dimension of brain functional network,” *Neural Plasticity*, vol. 2020, Article ID 8825547, 11 pages, 2020.